International Journal of Engineering & Technology, 8 (1.4) (2019) 249-256

International Journal of Engineering & Technology

Website: www.sciencepubco.com/index.php/IJET

Research paper



Performance Comparison of AHRS Algorithm for Quad Copter Application

Min-SeokJie[1], Da-Un Kim[2], Won-HyuckChoi[3*]

[2]Department of Aeronautical Systems Engineering
236-49, Gomseom-ro, Nam-myeon, Taean-gun,
32158Chungcheongnam-do, Republic of Korea
kdu0011@naver.com
[1,3]Department of Avionics Engineering Hanseo University
236-49, Gomseom-ro, Nam-myeon, Taean-gun,
32158Chungcheongnam-do, Republic of Korea
**Corresponding author E-mail: choiwh@hanseo.ac.kr*

Abstract

An Inertial Measurement nit (IMU) is an internal component of a device such as an unmanned aircraft, airplane, or satellite. Use an accelerometer, a gyro scope, and a ground magnetic meter to measure acceleration and torque. It's an integrated device that allows us to measure movement in three-dimensional space. In recent years when there are problems with receiving GPS signals from tunnels, indoors or electromagnetic interference, technologies such as navigation and others are being used to estimate locations such as IMU information. Accuracy and quick response are the most important requirements for all systems mentioned. Therefore, this paper compared the accuracy of the quaternion algorithm with the calculation speed based on the gradient descent method among the different solutions. The experiment used a quad cover to verify the estimated accuracy.

Keywords: IMU, Quad Copter, Quaternion, Madgwick algorithm, Mahony algorithm

1. Introduction

Quadr-copter is a variant of a traditional helicopter called a quadr-copter, and like an airplane, it is a multi-adjusted branch. The original helicopter was a rotary-wing helicopter consisting of a main rotor and a tail rotor. Quadcopter uses four identical rotors in place of the main rotor and the tail rotor to maximize safety and increase lift to achieve excellent transport capability. Currently, quadcopters are mostly applied to unmanned aerial vehicles (UAVs), which are popular for aerial shooting and hobby activities. The main advantage of a quadcopter is that its operating principles are very simple compared to conventional helicopter types, making it very easy to control [1].
Inertia sensors have many applications that convert the behavior of an object into electrical signals [1], [2]. Operating devices need the help of an inertia sensor. Inertia sensors are commonly referred to as sensors that measure different inertia, such as acceleration sensors and angular acceleration sensors. The acceleration sensor is capable of instantly detecting the acceleration and dynamic forces such as moving force and impact force acting on an object, so that it can be used for a wide range of vehicles, rail vehicles, aircraft, and ships [3]. Mechanical acceleration sensor that utilizes an inertia force, which is a half force due to acceleration, that measures the acceleration of inertia based on a stationary system is difficult to utilize due to complicated structure and has high reliability due to complicated structure [4]. On the other hand, silicon acceleration sensors have excellent mechanical properties of silicthree-dimensionalt reliability and mass production by using established semiconductor integrated circuit process technology and can miniaturize and make devices lighter [5].
The Attitude and Heading Reference System (AHRS), based on inertia sensors, is a system for measuring the posture of an object. The direction of a Euler angle, etc., is used as an expression of the posture [6]. To compensate for these measured positions, various algorithms have been applied, such as the Kalman Filter and the Complementary Filter. However, only Kalman filters and detailed filters based on the matrix are not efficient due to their high computational volumes and are limited in rotation due to the phenomenon of gimbal lock [6], [7]. However, the Quaternion rotation can prevent luggage loss because it has a different rotation method than Euler's angular rotation, and because the amount of yearly turnover is less than the matrix calculation, the system is less burdened. Therefore, this study compares the performance of quaternion - based algorithms for quad - copter. The performance of the Madgwick algorithm and the Mahony algorithm was tested in both static and dynamic states. Finally, we calculated the computation speed of the Kalman filter algorithm, the Madgwick algorithm and the Mahony algorithm to calculate the computation efficiency.

Copyright © 2019 Authors. This is an open access article distributed under the Creative Commons Attribution License, which permits unrestricted use, distribution, and reproduction in any medium, provided the original work is properly cited.

2. Quadcopter

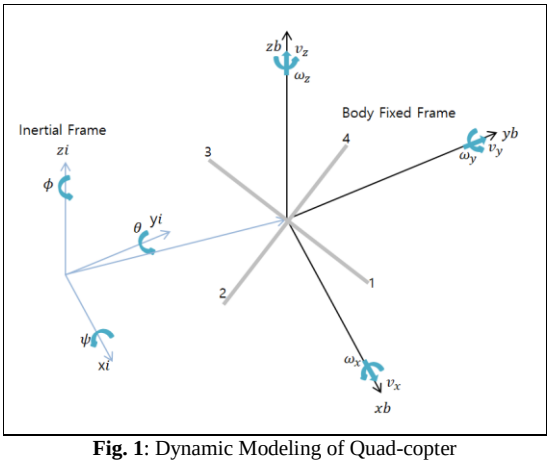


Fig. 1: Dynamic Modeling of Quad-copter

To model the dynamics of quadcopters, the gas coordinate system and the inertia coordinate system shall exist and shall represent the relationship between the two systems, as shown in Figure (1). This equation is expressed in a rotating matrix, as in Equation (2), with the following equation (1).

$$R_x(\varphi) = \begin{bmatrix} 1 & 0 & 0 \\ 0 & \cos\varphi & -\sin\varphi \\ 0 & \sin\varphi & \cos\varphi \end{bmatrix}$$
$$R_y(\theta) = \begin{bmatrix} \cos\theta & 0 & \sin\theta \\ 0 & 1 & 0 \\ -\sin\theta & 0 & \cos\theta \end{bmatrix} \quad (1)$$
$$R_z(\psi) = \begin{bmatrix} \cos\psi & -\sin\psi & 0 \\ \sin\psi & \cos\psi & 0 \\ 0 & 0 & 1 \end{bmatrix}$$

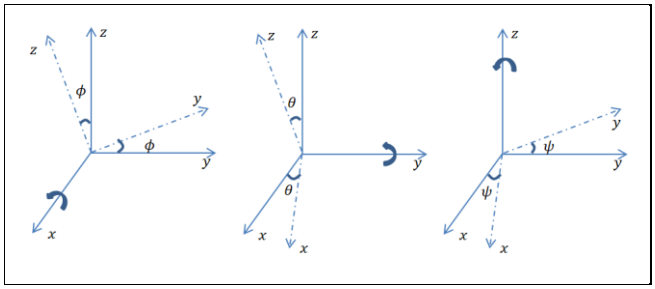


Fig. 2: Dynamic Modeling of Quad-copter

The rotational coordinate system for a fixed coordinate system is shown in Figure (2) as the rotation angle for each axis of rotation as it is fixed and rotated [8].

$$R_{zyx} = R_z(\psi)R_y(\theta)R_x(\varphi) = \begin{bmatrix} \cos\psi\cos\theta & \cos\theta\sin\psi & -\sin\theta \\ \sin\varphi\sin\theta\cos\psi - \cos\varphi\sin\psi & \sin\varphi\sin\theta\sin\psi + \cos\varphi\cos\psi & \sin\varphi\cos\theta \\ \cos\varphi\sin\psi\cos\psi + \sin\varphi\sin\psi & \cos\varphi\sin\theta\sin\psi - \sin\varphi\cos\psi & \cos\varphi\cos\theta \end{bmatrix} \quad (2)$$

In addition, the position of the quadcopter and Euler angles, such as expression (3) in the inertia coordinate system, can be represented with values of speed and acceleration, as in expression (4) in the gas coordinate system.

$$p = \begin{bmatrix} x \\ y \\ z \end{bmatrix}$$
$$\vartheta = \begin{bmatrix} \varphi \\ \theta \\ \psi \end{bmatrix} \quad (3)$$
$$v = \begin{bmatrix} v_z \\ v_y \\ v_x \end{bmatrix}$$
$$\omega = \begin{bmatrix} \omega_z \\ \omega_y \\ \omega_x \end{bmatrix}$$
$$\dot{P} = Rv \,,\, \omega = C\dot{\theta} \quad (4)$$

In Equation 4, R represents a matrix for converting the gas coordinate system relative to the inertia coordinate system. C is a matrix that represents the relationship between the inertia coordinate system and the velocity component of the Euler angle and the angular velocity vector of the gas coordinate system. Differentiating the equation 4 is as follows in Equation 5.

$$\begin{aligned} \ddot{p} &= R\dot{v} + \dot{R}v = R(\dot{v} + \omega \times v) \\ \dot{\omega} &= C\ddot{\vartheta} + \dot{C}\dot{\vartheta} \\ \dot{R}v &= \omega \times Rv \end{aligned} \tag{5}$$

Matrix C, which represents the relationship between the inertia coordinate system and the velocity component of the Euler angle and the angular velocity vector of the gas coordinate system, can lead to an equation, as shown in Equation 6, and is expressed in Equation 7 if C is differentiated again.

$$C = \begin{bmatrix} 1 & 0 & -\sin\theta \\ 0 & \cos\varphi & \sin\varphi\cos\theta \\ 0 & -\sin\varphi & \cos\varphi\cos\theta \end{bmatrix} \tag{6}$$

$$\dot{C} = \begin{bmatrix} 0 & 0 & -\dot{\theta}\cos\theta \\ 0 & -\dot{\varphi}\sin\varphi & \dot{\varphi}\cos\varphi\cos\theta - \dot{\theta}\sin\varphi\sin\varphi \\ 0 & -\dot{\varphi}\cos\varphi & -\dot{\varphi}\sin\varphi\cos\theta - \dot{\theta}\cos\varphi\sin\theta \end{bmatrix} \tag{7}$$

In addition, Newton's second law uses the laws of force and moment conservation on the gas to achieve the following equation.

$$\Sigma F = ma \rightarrow F + F_g = m\dot{v} + \omega \times (mv) \tag{8}$$

$$\Sigma M = \dot{H} \rightarrow Q - Q_G = I\dot{\omega} + \omega \times (I\omega) \tag{9}$$

m represents the mass of the gas, the moment of inertia of the gas is I, the moment of inertia of the airplane is F_g is the force of acceleration, the $\omega \times$ mv is the Euler equation for the moment, M The moment of inertia I is expressed as in equation 10, and the gas in the quad-copter is linear, indicating $I_{xx} = I_{yy}$.

$$I = \begin{bmatrix} I_{xx} & 0 & 0 \\ 0 & I_{yy} & 0 \\ 0 & 0 & I_{zz} \end{bmatrix} \tag{10}$$

Where F_g is the gravitational force acting on the airplane, which shall be represented in the airplane coordinate system, and the gravitational vector value ($g^o = [0 \quad 0 \quad -g]^T, g = 9.8$) expressed in the inertia coordinate system as follows : In addition, the Q_G is a gyro imperfection and can define from the following expressions from the four rotor angular rates of the quadcopter, Ω_2 , Ω_3, and Ω_4 :

$$Q_G = \omega \times I_R\Omega_G. \tag{11}$$

In Equation 11, I_R can represent the rotor's moment of inertia: $\Omega_g = [0\ 0\ \Omega_1 - \Omega_2 + \Omega_3 - \Omega_4]^T$. F and Q are the forces and moments applied to control quadcopters, so that the angular velocity of each of the four quadcopters is equal to Equation 12.

$$F = [0 \quad 0 \quad F_1 + F_2 + F_3 + F_4]^T \tag{12}$$

If the aircraft fixed coordinate system of the quadcopter is shown in Fig 1, the distance of the motor from the centre of gravity is l, and the torque factor λ to thrust is given as shown in Fig. 2, the hammer

$$T = T_1 + T_2 + T_3 + T_4 \tag{13}$$

$$\begin{aligned} \tau_\varphi &= lT_3 + lT_4 - lT_2 - lT_2 \\ \tau_\theta &= lT_1 + lT_4 - lT_2 - lT_3 \\ \tau_\psi &= \lambda T_1 - \lambda T_2 + \lambda T_3 - \lambda T_4 \end{aligned} \tag{14}$$

If the quad has the same thrust, it will fly in place and can be controlled in the direction of Pitch, Roll, and Yaw, depending on the force applied by the torque, as shown in Figure 3 [9], [10].

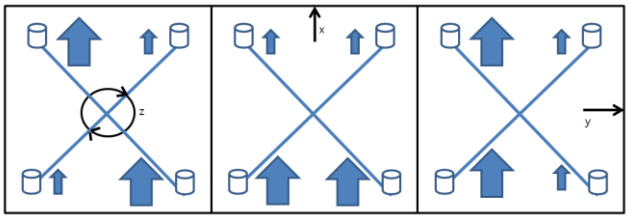


Fig. 3: Direction of Quadcopter for Motor Rotation

3. Position measuring system

The Attitude Heading Reference System (AHRS) is a three-axis sensor system that provides the three-dimensional position information direction (Yaw, Pitch and Roll) in real time. AHRS ' main function provides directional data. The AHRS consists of a decider system, accelerometer, and gyroscope on all three axes and creates a system that can measure the position of objects in 3D space [11].
The basic technique for calculating AHRS systems is based on direct measurement of AHRS sensors. Several technologies were then developed to improve the error correction and calculation process of AHRS. These techniques include the Kalman filter algorithm, the Mahony algorithm, or the Madgwick algorithm. Among these techniques, the Madgwick algorithm and the Mahony algorithm have two or more axes in the 3D space.

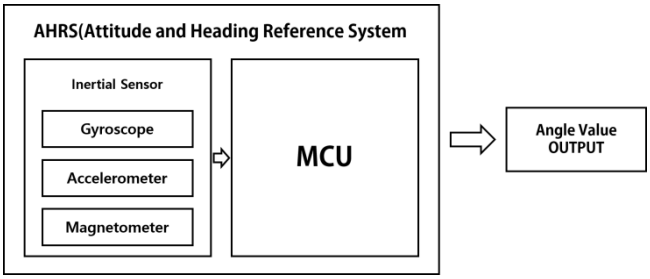


Fig. 4: Position measuring system

3.1 Quaternion Data

The Quaternion is a system of numbers extended from the original number introduced by Irish mathematician William Rowan Hamilton in 1843. Quaternion perform well in the rotation or orientation of an object. Quaternion are used to overcome various problems, such as gimbal locks, arising from the computation of Euler Angles. In addition, compared to a rotating matrix using nine elements, it can be described briefly in four elements.

Table 1: Matrix vs. Quaternion

Category	Matrix	Quaternion
Amount of data	float 16 EA	float 4EA
Calculation rate	float Cross 16*16Time	float Cross 16 Time
Quality of result	Error such as luggage trap	Settlement of the burden

Quaternion are mathematically expressed as in equation (15), where q0, q1, q2, q3 and q are all mistakes. It is generally known that three priors cantered on another axis defined by Euler angles can be replaced by one around a vector in the reference frame. The Quaternion can describe the rotation right away.

$$q = q_0 + q_1 i + q_2 j + q_3 k \tag{15}$$

$$q = [q_0 q_1 q_2 q_3]^T \tag{16}$$

The two quotas on data, p and q, are produced using the Kronecker product, marked as $\otimes$. The two rotations are then shown as $\otimes$. rotations.

$$p \otimes q = \begin{bmatrix} p_0 q_0 & -p_1 q_1 & -p_2 q_2 & -p_3 q_3 \\ p_0 q_1 & +p_1 q_0 & +p_2 q_3 & -p_3 q_2 \\ p_0 q_2 & -p_1 q_3 & +p_2 q_0 & -p_3 q_1 \\ p_0 q_3 & +p_1 q_2 & -p_2 q_1 & -p_3 q_0 \end{bmatrix} \tag{17}$$

The data for the two quaternions are not subject to the exchange law.

$$p \otimes q \neq q \otimes p \tag{18}$$

Size of the Quaternion (Magnitude)

$$Magnitude(q) = || \, q \, || = \sqrt{q_0^2 + q_1^2 + q_2^2 + q_3^2} \tag{19}$$

Conjugation of Quaternion

$$Conj(q) = q^* = [q_0 - q_1 - q_2 - q_3]^T \tag{20}$$

Inverse (reciprocal) of the quorum

$$\in v(q) = q^{-1} = \frac{q^*}{||q||^2} \tag{21}$$

Normalization of the Quaternion

$$Normalize(q) = \left[\frac{q_0}{||q||}\ \frac{q_1}{||q||}\ \frac{q_2}{||q||}\ \frac{q_3}{||q||}\right]^T \tag{22}$$

So, if you look at it in 3D vector rotation,

$$\vec{w} = q \otimes \begin{bmatrix}0\\ \vec{v}\end{bmatrix} \otimes q^* \tag{23}$$

$$q = \begin{bmatrix}\cos(\psi/2)\cos(\theta/2)\cos(\Phi/2) + \sin(\psi/2)\sin(\theta/2)\sin(\Phi/2)\\ \cos(\psi/2)\cos(\theta/2)\sin(\Phi/2) - \sin(\psi/2)\sin(\theta/2)\cos(\Phi/2)\\ \cos(\psi/2)\sin(\theta/2)\cos(\Phi/2) + \sin(\psi/2)\cos(\theta/2)\sin(\Phi/2)\\ \sin(\psi/2)\cos(\theta/2)\cos(\Phi/2) - \cos(\psi/2)\sin(\theta/2)\sin(\Phi/2)\end{bmatrix} \tag{24}$$

Therefore, the equation for the angle of yaw, pitch, and Roll is as follows.

$$\begin{bmatrix}\psi\\ \theta\\ \Phi\end{bmatrix} = \begin{bmatrix}atan(2(q_1q_2 + q_0q_3)/(q_0^2 + q_1^2 - q_2^2 - q_3^2))\\ asin(2(q_0q_2 - q_3q_1))\\ atan(2(q_0q_1 + q_2q_3)/(q_0^2 - q_1^2 - q_2^2 + q_3^2))\end{bmatrix} \tag{25}$$

3.2 Kalman Filter Algorithm

Kalman Filter is used in a wide range of fields, especially in the use of sensors to correct errors or to mix sensors. Kalman Filter is an algorithm that best estimates input values, including irregular deviations, is a statistical method presented by R. E. Kalman to solve the problem of discrete linear filters. The Kalman Filter estimates the optimal performance for a linear system with white noise, which is a Gaussian Distribution, which is an expansion of the system model and the observational model.
The Kalman filter uses measurement data and new measurement data to control the noise contained in the data, and thus has linear movements with algorithms that use it to estimate new results.
In the forecasting phase, the state is obtained by directly integrating the gyro scope measurement and the predicted covariance matrix is obtained based on the variance of the measured value. In the update phase, the measurement covariance matrix is updated based on the measurement reliability of the accelerometer and the force meter values. Measurement will be unreliable if there is a rapid movement or if there is a problem with the magnetic field.

3.2.1 Quaternion Position Measurement System Model

When estimating self-disaggregation by applying the postural measurement system model, the Kalman filter algorithm can be used to implement the filtering process of observed data from sensor measurements and estimated values over time. The linear system model and the observational model for posture measurements are expressed in the form of discrete differential equations, the same as the equation (26) and (27), and A is the matrix of systems that are the core of the posture estimation algorithm [12]. In equation (26), the flight attitude measuring system model, is the status variable represented by the Quaternion at time k. ω k is the noise model of the state variable, which is subsequently represented by the covariance matrix of Q, which affects the prediction of the covariance of the system model. In equation (27), the observational model of the sensor, the zk represents the measurement and the H matrix represents the estimate of the measurement along with the status variable. A burst is a Gaussian random noise in the measurement and is subsequently represented by a covariance matrix of R, which affects the gain estimate.

$$x_{k+1} = Ax_k + w_k \tag{26}$$

$$z_k = Hx_k + v_k \tag{27}$$

The system matrix (A) changes because it contains angular velocity measurements, not constants. The status variable (x) of the system model is expressed as a Quaternion, as shown in equation (28), and converted to the quadrant using Euler angles calculated by the above method (29).

$$x = \begin{Bmatrix}q_0\\ q_1\\ q_2\\ q_3\end{Bmatrix} \tag{28}$$

$$\begin{Bmatrix}q_0\\ q_1\\ q_2\\ q_3\end{Bmatrix} = \begin{Bmatrix}\cos(\psi/2)\cos(\theta/2)\cos(\Phi/2) + \sin(\psi/2)\sin(\theta/2)\sin(\Phi/2)\\ \cos(\psi/2)\cos(\theta/2)\sin(\Phi/2) - \sin(\psi/2)\sin(\theta/2)\cos(\Phi/2)\\ \cos(\psi/2)\sin(\theta/2)\cos(\Phi/2) + \sin(\psi/2)\cos(\theta/2)\sin(\Phi/2)\\ \sin(\psi/2)\cos(\theta/2)\cos(\Phi/2) - \cos(\psi/2)\sin(\theta/2)\sin(\Phi/2)\end{Bmatrix} \tag{29}$$

Thus, the system model can be expressed as an expression (30) of the quaternion as a medium for measurements of angular velocity.

$$\begin{Bmatrix}\dot{q_0}\\ \dot{q_1}\\ \dot{q_2}\\ \dot{q_3}\end{Bmatrix} = \begin{bmatrix}0 & -a_x & -a_y & -a_z\\ a_x & 0 & a_z & -a_y\\ a_y & -a_z & 0 & a_x\\ a_z & a_y & -a_x & 0\end{bmatrix} \begin{Bmatrix}q_0\\ q_1\\ q_2\\ q_3\end{Bmatrix} \tag{30}$$

The system model of the above attitude measurements can lead to linear integration of discrete systems in equation (31), and whether the attitude of the flight is expressed in quatrains or in physical angles.

$$\begin{Bmatrix} q_0 \\ q_1 \\ q_2 \\ q_3 \end{Bmatrix}_{k+1} = \begin{Bmatrix} q_0 \\ q_1 \\ q_2 \\ q_3 \end{Bmatrix}_{k} + \Delta t \bullet \begin{Bmatrix} \dot{q_0} \\ \dot{q_1} \\ \dot{q_2} \\ \dot{q_3} \end{Bmatrix}_{k} = \left(I + \Delta t \bullet \frac{1}{2} \begin{bmatrix} 0 & -a_x & -a_y & -a_z \\ a_x & 0 & a_z & -a_y \\ a_y & -a_z & 0 & a_x \\ a_z & a_y & -a_x & 0 \end{bmatrix} \right) \begin{Bmatrix} q_0 \\ q_1 \\ q_2 \\ q_3 \end{Bmatrix}_{k} \tag{31}$$

In the above equation, the system model matrix (A) is organized as shown in the following equation (32) and can only be applied to the postural measurement card filter algorithm.

$$A = I + \Delta t \bullet \frac{1}{2} \begin{bmatrix} 0 & -p & -q & -r \\ p & 0 & r & -q \\ q & -r & 0 & p \\ r & q & -p & 0 \end{bmatrix} \tag{32}$$

3.2.2 Prediction process

The forecasting process is the process of predicting how the current data will change from the previous data, following expressions (33) and expressions (34).

$$\hat{x}_k^- = A\hat{x}_{k-1} \tag{33}$$

$$P_k^- = AP_{k-1}A^T + Q \tag{34}$$

In the above equation, ' - ' indicates the predicted value and ' ^ ' indicates the estimated value. Therefore, in the prediction process, estimate how the estimate $\hat{x}_k$ changes when the time changes from t_k to t_{k+1}, and receive the last estimate $\hat{x}_{k-1}$ and Outputs the predicted value $\hat{x}_k^-, P_k^-$, A and Q are system model variables used in the forecasting process.

3.2.3 Estimation process

The estimation process is the process of obtaining the current estimated value using the estimated values and measurements z_k obtained from the previous prediction process, as shown in the following equation (35), (36), and (37).

$$K_k = P_k^- H^T (HP_k^- H^T + R)^{-1} \tag{35}$$

$$\hat{x}_k = \hat{x}_k^- + K_k(z_k - H\hat{x}_k^-) \tag{36}$$

$$P_k = P_k^- - K_k H P_k^- \tag{37}$$

In the above equation, K determines the weight between the measurement and the estimate by benefiting only the knife. Z_k is a measured value that contains information obtained from sensors, etc. Therefore, the estimation process receives the predicted value $\hat{x}_k^-, P_k^-$ and the measured value Z_k as input values to obtain the estimated value $\hat{x}_k$ and the error covariance P_k. Error covariance indicates how different the estimate of the Kalman Filter is from the true value. This means that the error covariance is a measure of the accuracy of the estimate. The values H and R are system model variables used in the estimation process.

3.3 Madgwick Algorithm

This algorithm incorporates magnetic distortion compensation and can use the Quaternion representation to calculate accelerometer and magnetic meter data analytically and with the optimized gradient decent algorithm. Figure 5 shows a block diagram of the implemented filters.

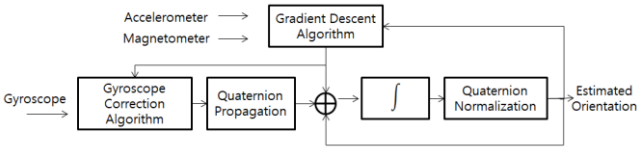


Fig. 4: Madgwick Algorithm Block Diagram

The direction of the quadcopter is calculated through two main processes. First, gyroscope measurements are calculated using a calibration algorithm determined by parameter. to minimize the effects of bias and drift error. Used to calculate the direction of the quadcopter starting with the estimated direction in the previous step. The accelerometer and the force meter measurements are then fused with the adjustable parameter β through the graduate decent algorithm and only the output of the graduate decent algorithm is considered using the expected output.

3.3 Mahony Algorithm

The Mahony algorithm is also called a nonlinear upper-filter algorithm and reconfigures direct measurements such as the direction of gravity or the direction of the magnetic field obtained from the IMU. This algorithm is ideal for embedded hardware platform configurations

because of its low complexity. In addition, it can avoid the possible peak lock when the equivalent rotation of the estimated four won is close to 90 degrees.

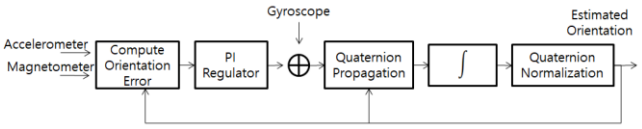


Fig. 5: Mahony Algorithm Block Diagram

Figure 5 above is a block diagram of the Mahony algorithm. A bearing error is obtained from data on the direction of posture of the quadcopter, measured in the previous stage of the algorithm, and a calibration step based on the PI compensation device is used to compensate for the measured angular velocity. Next, the Quaternion wave is integrated to obtain estimates of the direction after the normal quota normalization.

4. Test Results

The results below show that the Quaternion-based algorithm is a real-time result graph of the Madgwick algorithm and the Mahony algorithm. The sensor used in the experiment was the MPU 9250 IMU sensor, and the board used was used to collect experimental data using the Arduino Board. Figures (6) and (8) were tested assuming that the quadcopter is dynamic, and a slight overshoot occurs in the Mahony algorithm. The two algorithms showed similar results. However, in the static state of the figures (7) and figures (9), some noise was observed in the Mahony algorithm.

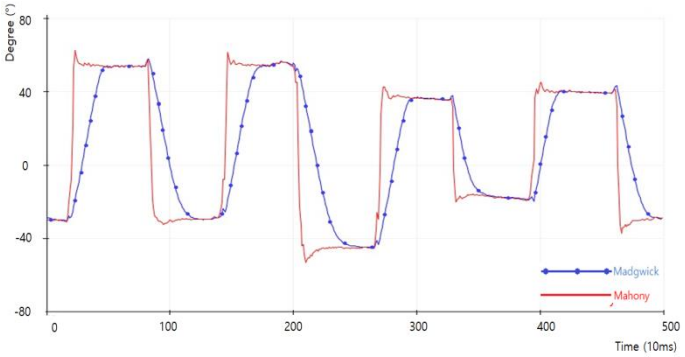


Fig. 6: Dynamic Roll Angle

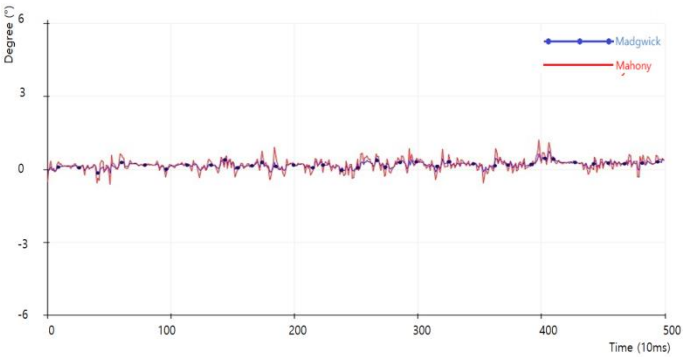


Fig. 7: Static Roll Angle

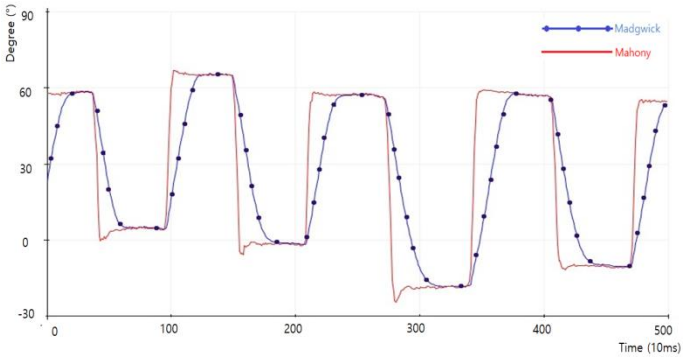


Fig. 8: Dynamic Pitch Angle

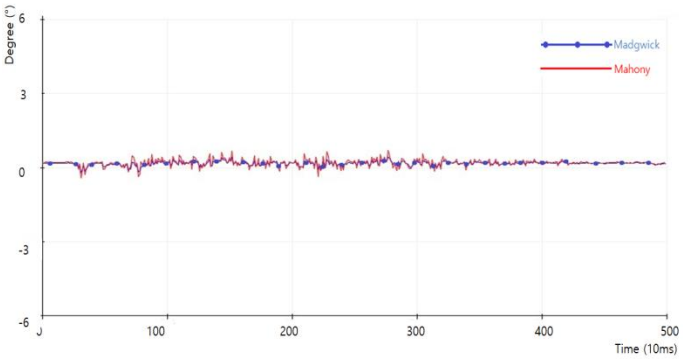


Fig. 9: Static Pitch Angle

With further analysis, comparisons were made on the calculation speed of the algorithms presented in this thesis. This experiment was performed in the Matlab environment of the Intel-quadrated processor. The tic-toc function in Matlab was used to calculate the running time of the loop estimating the quadcopter position. Table 2 below is the result of the calculation speed experiment. As you can see from the results, the Quaternion-based Madgwick algorithm and the Mahony algorithm are about 11 to 13 times faster than the Kalman Filter algorithm.

Table 2: Algorithm calculation speed

Algorithm	Calculation Speed[ms]
Kalman	0.236
Madgwick	0.02
Mahony	0.0186

5. Conclusion

With the development of IMU sensors, IMU sensors are being used in various fields. Although accurate data can be obtained by using expensive sensors, it increases price of sensors. Therefore, data can be applied to AHRS using low cost IMU sensor to increase reliability. Currently, the Kalman Filter algorithm is used primarily for data calibration of IMU sensors. However, only Kalman filters and detailed filters based on the matrix are not efficient due to their high computational volumes and are limited in rotation due to the phenomenon of gimbal lock. Therefore, in this paper, the Madgwick algorithm, which is a Quaternion -based algorithm, was compared with the Mahony algorithm. When the quad copter was rotated at pitch and rolls angles, the speed was slightly faster than the Mahony filter, but a slight overshoot occurred. Further analysis also compared the calculation speed with the Kalman Filter algorithm, and found that the calculation speed was between 11 and 13 times faster. Therefore, a quaternion-based algorithm can be applied to quad-copter.

References

[1] Zhang, X., Yang, Z., Zhang, T., & Shen, Y. “An improved Kalman filter for attitude determination of multi-rotor UAVs based on low-cost MEMS sensors”. In Guidance, Navigation and Control Conference (CGNCC), pp.407-412, 2016 IEEE Chinese.
[2] H. G. Min "Design of Complementary Filter using MEMS-type Gyroscope and Accelerometer”, Changwon University, (2011).
[3] W. S. Jo, "A Study of a Calibration method and Flight Test for MEMS Sensor”, Korea Aviation University, (2017).
[4] D. H. Cho, " Design and control of a quad-rotor UAV " KAIST (2009).
[5] Y. H. Ok, " Implementation on the Attitude Controller of the Quad-rotor using DSP " Hoseo University (2015).
[6] Pham, S. T., and Chew, M. T. “Sensor signal filtering in quadrotor control”, In Sensors Applications Symposium, (2014), pp.293-298.
[7] H. S. Kim, “A Design of Hovering System for Quadrotor UAV using Multi-Sensor Fusion” Seo-kyeong University (2016).
[8] J. S. Kim, “The Simulator for Control of Quad copter using sensor combination” Dong-A University, (2012).
[9] S. Y. Hwang, J. H. Park and J. M. Lee, “Detection of Inclination for Quadcopter's Landing Position Control.” Institute of Control, Robotics and Systems, (2010), pp. 35-38.
[10] Y. J, You and J. R. Ryoo, " Geomagnetic Sensor Compensation and Sensor Fusion for Quadrotor Heading Direction Control ". Journal of The Institute of Electronics and Information Engineers., vol. 53, no. 7, (2016), Pp. 95-102.
[11] S. K. HAN, I. H. LEE and N.R. Park, “Reliability of static balance abilities measure using a smartphone`s acceleration sensor”, Journal of the Korea Academia-Industrial Cooperation Society., vol. 17, no. 6, (2016), pp. 233-238.
[12] M.D. S. Rahman, C. H. Choi, S. K. Kim, I. D. Park and Y. P. Kim, “Noise-robust electrocardiogram R-peak detection with adaptive filter and variable threshold”, Journal of the Korea Academia-Industrial Cooperation Society., vol. 18, no. 12, (2017), pp. 126-134.
[13] K. S. Ryu, B. K. Kim, D. J. Kim, M. S. Jang, H. S. Ko and HC Kim, “A State-of-Charge estimation using extended Kalman filter for battery of electric vehicle”, Journal of the Korea Academia-Industrial Cooperation Society., vol. 18, no. 10, (2017), pp. 15-23.